Journal of Applied Mathematics and Physics (ZAMP)
Vol. 28, 1977 Birkhäuser Verlag Basel

Instabilities of Longitudinal Convection Rolls in Couette Flow

By R. M. Clever and F. H. Busse, Institute of Geophysics and Planetary Physics, and R. E. Kelly, Mechanics and Structures Dept, University of California, Los Angeles, California, USA

Dedicated to Professor Nikolaus Rott on the occasion of his 60th birthday.

1. Introduction

Although the study of the onset and development of thermal convection in shear flows dates back to the 1920's, interest in the topic continues to be high due to its importance in several distinct fields of research. In a review by Kelly [1], 43 of the references listed were found to have been published within the past ten years. Many of these, however, were related to the prediction of linear stability theory that, at low Reynolds numbers, the preferred mode of convection consists of longitudinal rolls or vortices which are spatially periodic in a direction normal to the plane of the flow and whose axes are in the direction of the flow. (This prediction holds for a unidirectional flow with a horizontally constant vertical temperature gradient imposed on it and with no side-walls.) Knowledge concerning possible secondary instabilities of the rolls as the Reynolds (*Re*) or Rayleigh (*Ra*) number increases is still scanty, although the original observation of such a possible instability was made in 1937 by Avsec [2] for the case of a channel flow over a heated plate. In fact, the single relevant theoretical investigation has been made only recently by Clever and Busse [3], for the case of free convection flow in an inclined layer. They obtained satisfactory agreement with the experimental results of Hart [4], who observed in that case the onset of waviness in the rolls as *Ra* increases for a fixed angle of inclination. In this paper, theoretical prediction of the onset of waviness in the rolls is made for the case of Couette flow when heated from below. Although this problem is somewhat similar to the instability of Taylor vortices contained between concentric, rotating cylinders [5, 6], the governing equations are different due to three-dimensionality, even if the Prandtl number is taken to be unity in the convection problem.

Perhaps the most interesting application of results concerning thermal convection in a shear flow is to the appearance of cloud streets in the planetary boundary layer. The streets are formed by the advection of moist air upwards in the convergence region of roll vortices, as shown schematically in Fig. 1 (taken from the paper by Fleagle [7]). According to Kuettner [8], the spacing between cloud streets is 2–8 km, and they can extend up to 500 km in length. Kuettner presented data obtained in the tropics, where

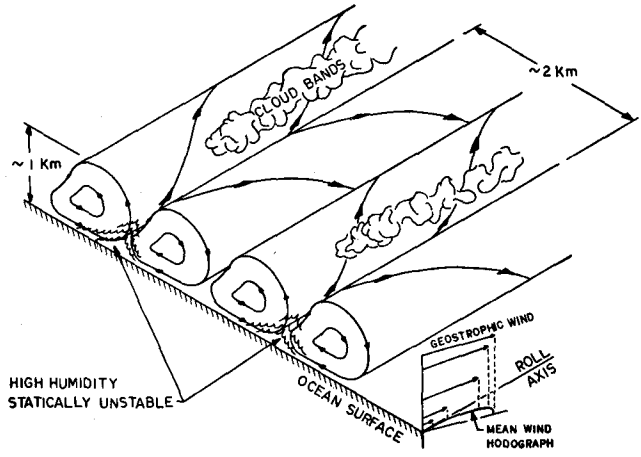

Figure 1
Schematic of flow in the planetary boundary layer, with longitudinal rolls giving rise to cloudstreets (from [7]).

the main forcing mechanism for the rolls is undoubtedly buoyancy. The rolls were found to be aligned in the mean wind direction, and the ratio of wavelength to inversion height was close to what one would predict on the basis of linear Rayleigh-Bénard convection theory. The very fact that organized structures were observed suggests that the mean effects of turbulence can be simulated by an eddy viscosity. Krishnamurti [9] has discussed in detail the occurrence of cellular convection in the atmosphere on this basis.

In regions away from the tropics, the Coriolis force can be important for the occurrence of the rolls, both in its effect upon the mean velocity profile and in including instability (cf. [10]). In a study of field data collected in the USA, LeMone [11] concluded that the observed structure of the atmospheric rolls was similar to that predicted on the basis of Ekman layer stability analyses. However, she concluded that buoyancy is also important from measurements of the magnitude and aspect ratio of the rolls. In general, therefore, both rotation and stratification should be considered when modelling atmospheric rolls.

Because we are concerned in this paper with three dimensional aspects caused by the instability of longitudinal convection rolls, observation of regular three dimensional structures in atmospheric rolls are of particular interest. If correlation can be made between any such structure and our theoretically predicted waviness for the convection rolls, then the use of a turbulent eddy viscosity to correlate theoretical and experimental results with atmospheric phenomena would be justified to a far greater extent than is presently felt to be acceptable. The waviness of the longitudinal rolls is associated with the same Reynolds stress terms which are responsible for the turbulent stresses simulated by an eddy viscosity. Hence, a positive correlation would indicate a

clear separation between the small scale atmospheric motions causing dissipation and the larger scales which enter the dynamics in much the same way as in laboratory experiments.

At the present time, the evidence of such a correlation is far from being conclusive. In part, this is due to the fact that the atmospheric rolls are observed to have various kinds of three-dimensional structures. For instance, Malkus and Riehl [12, p. 45] report in their study of cloud streets in the tropical Pacific that 'several scales of organization were frequently encountered, and in some disturbed regions a double organization was suspected, with some portions of the parallel cloud lines greatly amplified at periodic intervals along the rows . . .' Kuo [13] has suggested that this modulation is due to the simultaneous occurrence of disturbances within the convective zone which are periodic in the mean flow direction and which propagate along the rolls. However, the same effect could be induced by internal gravity waves or Kelvin–Helmholtz waves occurring above the inversion. A much smaller scale structure is also often observed. For instance, Kuettner [14] states that most cloud streets are composed of individual cumuli 'lined up like pearls on a string' (see Fig. 13 of [8] for a good example). It is very doubtful if such a structure can be associated with the instability discussed here. However, Markson [15] has measured longitudinal variations in clear air convective rolls with a scale of about 1.6 times the wavelength of the basic rolls. Such a scale is at least consistent with our theoretical predictions, and so a correlation might exist in this case. More detailed observations of the structure of the velocity field in the atmospheric convection rolls would certainly be very desirable.

We proceed now to the analysis of the Couette flow problem.

2. The Basic State

We consider the motion induced in a Boussinesq fluid contained between two plane, solid horizontal boundaries (of infinite extent and separated by the distance H) which are moving oppositely to each other in the x-direction with a velocity difference ΔU_0^*. The fluid is heated from below so that a constant temperature difference ΔT_0^* exists across the layer. Dimensional velocity components in the x (streamwise), y (cross-stream), and z (vertical) directions are denoted by u^*, v^*, and w^*, respectively.

The basic steady state, whose stability we consider later, is composed of linear velocity and temperature variations (corresponding to strictly laminar flow) plus the deviations from such variations caused by the longitudinal rolls. These rolls will occur as soon as $Ra > Ra_c$, the critical Rayleigh number without shear ($=1707.8$), and they are well-known to be the preferred form of convection for reasonably small Reynolds numbers (cf. [16]). The rolls are independent of the x-coordinate, and so a stream function (Ψ) can be used to describe the flow in the (y, z) plane. The basic state is then represented as

$$U^* = \Delta U_0^* U(y, z) = \Delta U_0^* \{z + U_1(y, z)\}, \tag{2.1}$$

$$V^* = (\kappa/H)V = (\kappa/H)\frac{\partial \Psi}{\partial z}, \qquad W^* = (\kappa/H)W = -(\kappa/H)\frac{\partial \Psi}{\partial y}, \tag{2.2a, b}$$

$$T^* = \Delta T_0^* \{-z + \Theta(y, z)\}, \tag{2, 3}$$

where κ is the thermal diffusivity and the lengths are nondimensionalized with respect to H. The origin of z in the following is taken to be mid-way between the boundaries.

The x-momentum equation is then

$$\frac{1}{Pr}\left\{\frac{\partial \Psi}{\partial z}\frac{\partial U_1}{\partial y} - \frac{\partial \Psi}{\partial y}\left(1 + \frac{\partial U_1}{\partial z}\right)\right\} = \frac{\partial^2 U_1}{\partial z^2} + \frac{\partial^2 U_1}{\partial y^2} \tag{2.4}$$

where Pr is the Prandtl number. The equation for Ψ is obtained by eliminating pressure from the y- and z-momentum equations and is

$$\frac{1}{Pr}\left\{\frac{\partial \Psi}{\partial z}\frac{\partial}{\partial y}(\nabla^2 \Psi) - \frac{\partial \Psi}{\partial y}\frac{\partial}{\partial z}(\nabla^2 \Psi)\right\}$$

$$= -Ra\frac{\partial \Theta}{\partial y} + \nabla^4 \Psi \tag{2.5}$$

The energy equation is

$$\frac{\partial \Psi}{\partial z}\frac{\partial \Theta}{\partial y} + \frac{\partial \Psi}{\partial y}\left\{1 - \frac{\partial \Theta}{\partial z}\right\} = \nabla^2 \Theta \tag{2.6}$$

The boundary conditions are

$$U_1 = \frac{\partial \Psi}{\partial y} = \frac{\partial \Psi}{\partial z} = \Theta = 0 \tag{2.7}$$

at $z = \pm\frac{1}{2}$.

It is clear that Eqns. (2.5, 2.6) can be solved independently of (2.4). These can be solved just as in the case of two-dimensional convection rolls without a mean flow. The actual method used to solve these equations is the same Galerkin technique explained in detail by Clever and Busse [17]. The wavelength of the rolls is assumed to be the critical wavelength for the onset of Rayleigh-Bénard convection. Once Ψ is determined as a function of Ra and Pr, $U_1(y, z)$ can be determined from the linear, inhomogeneous equation (2.4), using a similar method. We note that U_1 is strongly dependent upon Pr. Its qualitative dependence upon Ra is revealed by noting that near Ra_c, where $\Psi \sim 0$ $(Ra\text{–}Ra_c)^{1/2}$, U_1 is given approximately by

$$-\frac{1}{Pr}W = \frac{\partial^2 U_1}{\partial z^2} + \frac{\partial^2 U_1}{\partial y^2}, \tag{2.8}$$

and it is clear that the average of U_1 with respect to y is zero. In this limit, U_1 is produced solely through vertical advection by the rolls of the mean vorticity associated with the Couette component. If we define

$$U_1(y, z) = \bar{U}_1(z) + \tilde{U}_1(y, z), \tag{2.9}$$

where an overbar denotes an average with respect to y, then in general the equation for $\bar{U}_1(z)$ is

$$\frac{d^2\bar{U}_1}{dz^2} = -\frac{1}{Pr}\frac{d}{dz}\overline{(\tilde{U}_1 W)}, \tag{2.10}$$

which yields a nonzero $\bar{U}_1$. The total mean flow, i.e., $z + \bar{U}_1$ is shown in Fig. 2 for the

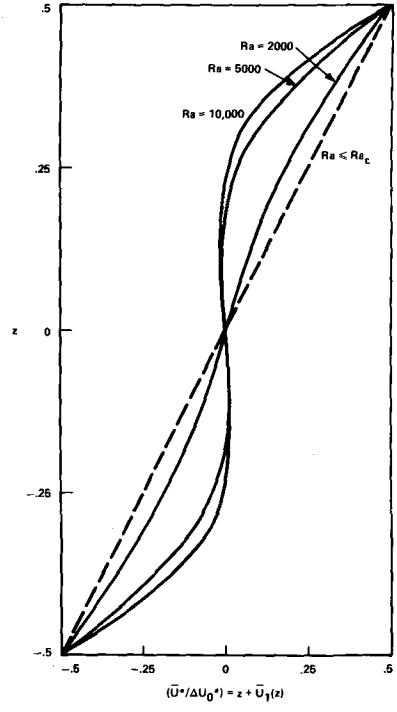

Figure 2
The mean flow profile when longitudinal rolls are present, for various Rayleigh numbers (Ra) and $Pr = 0.7$.

case of air ($Pr = 0.7$) and various values of Ra. At $Ra = 10{,}000$, a pronounced boundary layer structure is seen, with a nearly uniform velocity core. This feature was found earlier by Lipps [18] in his calculation for $Ra = 20{,}000$ and $Pr = 0.7$ (see his Fig. 10). For the same value of Ra but $Pr = 9.35$, Lipps found the deviation from a linear profile to be very small. The emergence of the boundary layers obviously affects the mean shear stress exerted at the walls. The increase in the mean wall shear stress, relative to the Couette value, is shown in Fig. 3 as a function of $(Ra–Ra_c)$. The effect would be even greater for smaller Pr.

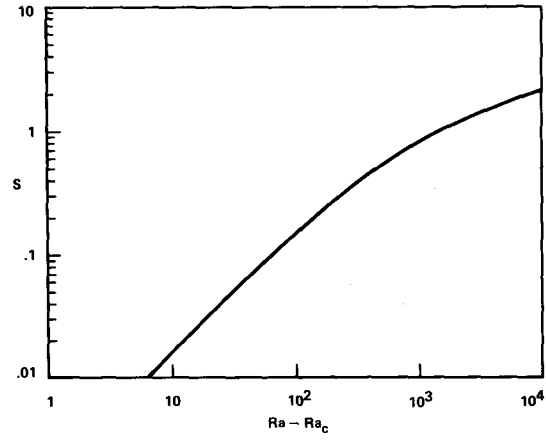

Figure 3
The increase in the average wall shear stress, $S = (\bar{\tau}_w H/\mu \Delta U^*) - 1$, as a function of Ra for $Pr = 0.7$.

3. The Stability Analysis

We now perturb the basic finite amplitude state just discussed by a small disturbance which depends on x and time, as well as y and z. For time, we introduce the diffusive scaling

$$t^* = (H^2/\kappa)t \tag{3.1}$$

For the streamwise component of velocity, we let

$$U^* = \Delta U_0^*(z + U_1) + (\kappa/H)\tilde{\varepsilon}\tilde{U}(x, y, z, t), \tag{3.2}$$

where $\tilde{\varepsilon}$ is a small parameter. The diffusive scaling (κ/H) is introduced for the perturbation in order to retrieve the limiting case $\Delta U_0^* = 0$. The other velocity components are represented in the form

$$w^* = (\kappa/H)\{W_1 + \tilde{\varepsilon}\tilde{w}(x, y, z, t)\}, \tag{3.3}$$

etc., and a nondimensional perturbation velocity vector is introduced as

$$\mathbf{v} = \mathbf{i}\tilde{u} + \mathbf{j}\tilde{v} + \mathbf{k}\tilde{w}, \tag{3.4}$$

where $(\mathbf{i}, \mathbf{j}, \mathbf{k})$ are unit vectors in the (x, y, z) directions. The temperature is defined by

$$T^* = \Delta T_0^*\{-z + \Theta + \tilde{\varepsilon}\theta(x, y, z, t)\}. \tag{3.5}$$

The equations for the various disturbance quantities are obtained through linearization (for $\tilde{\varepsilon} \ll 1$) of the full equations. They are

$$\begin{aligned} &\frac{1}{Pr}\frac{\partial \mathbf{v}}{\partial t} + Re\, U\frac{\partial \mathbf{v}}{\partial x} + \frac{1}{Pr}\left\{V\frac{\partial \mathbf{v}}{\partial y} + W\frac{\partial \mathbf{v}}{\partial z}\right\} \\ &\quad + Re\,\mathbf{i}(\mathbf{v}\cdot\nabla U) + \frac{1}{Pr}\{\mathbf{j}(\mathbf{v}\cdot\nabla V) + \mathbf{k}(\mathbf{v}\cdot\nabla W)\} \\ &\quad = -\nabla\mathbf{p} + Ra\theta + \nabla^2\mathbf{v}, \end{aligned} \tag{3.6}$$

$$\frac{\partial\theta}{\partial t} + Re\,Pr\,U\frac{\partial\theta}{\partial x} + V\frac{\partial\theta}{\partial y} + W\frac{\partial\theta}{\partial z} + \frac{\partial\Theta}{\partial y}\tilde{v} + \left(-1 + \frac{\partial\Theta}{\partial z}\right)\tilde{w} = \nabla^2\theta, \tag{3.7}$$

$$\nabla\cdot\mathbf{v} = 0. \tag{3.8}$$

In the actual analysis, the solenoidal velocity vector is represented in the manner of Clever and Busse [17]. Rather complicated equations result which are not presented here. Both the equations and the ensuing analysis are very similar to those of the inclined layer problem [3].

Because the coefficients of the unknowns in Eqns. (3.6–3.8) are independent of x and t, any disturbance unknown, say, $\tilde{u}$, can be assumed in the form

$$\tilde{u}(x, y, z, t) = \hat{u}(y, z)\exp(ibx + \sigma t). \tag{3.9}$$

The growth rate σ is the eigenvalue for the system of Eqns (3.6–3.8). When amongst all disturbances (for given values of Re and Ra) the largest real part of σ exceeds zero, then the rolls are unstable. As in the case of an inclined layer [3], the disturbance equations allow modes with two different symmetries. Only one of these has been found to be unstable in the range of Re and Ra investigated. For the unstable mode, $\tilde{v}$ is a symmetric function of y, and so the instability appears to be 'sinuous' in a plan-view. Two different kinds of instability can then occur. The *wavy instability* is characterized by real σ, i.e., zero frequency[2]), whereas the imaginary part of σ ($=\sigma_i$) is nonzero for the *oscillatory instability*. The latter instability manifests itself by waves travelling in either direction along the convection rolls, with a wave velocity different from the mean flow velocity.

The neutral stability boundaries for these two instabilities are shown in Fig. 4 as a function of $(Ra–Ra_c)$ and Re for $Pr = 0.71$. For $Re = 0$, the oscillatory instability is predominant (at least for a longitudinal roll wave number of 3.117). Although this mode is destabilized as Re increases, the wavy mode is affected even more. For $Re > 39$, it is the predominant mode of instability if the shear flow is established before the Rayleigh number is increased much beyond Ra_c. However, if the shear flow is established only after the Rayleigh number has been increased initially to a value in region A (bounded by the dashed line and the two stability boundaries), then further increase in Ra will lead to an oscillatory instability, whereas a decrease in Ra will lead to a wavy instability. If Re is increased from zero for a fixed value of Ra in region A, then either instability can occur, depending upon the value of Ra. We also note, for $Re > 200$, the rolls become unstable for $(Ra - Ra_c) \simeq 57$, so that rather precise control over Ra would be required in an experiment in order to observe the transition.

The neutral curve of the wavy instability corresponds to the limit of $b \to 0$. Figure 5 shows a typical graph of the dependence of the growth rate σ upon b. The wave number b of the most unstable disturbance increases rapidly once Ra has exceeded the

[2]) For our antisymmetric mean flow.

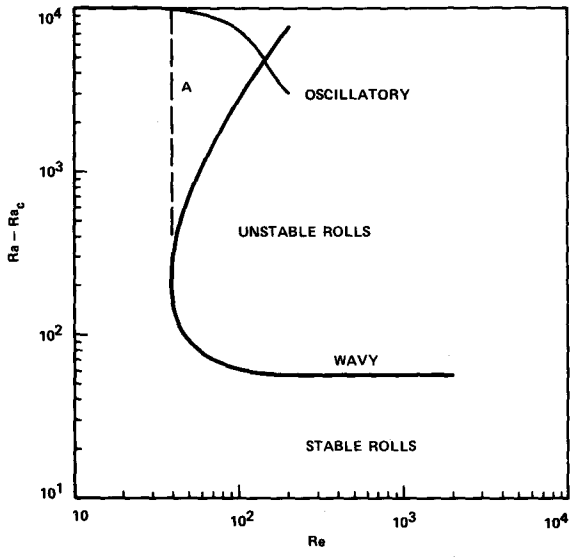

Figure 4
The neutral stability boundaries for the wavy and oscillatory instabilities in Couette flow, for $Pr = 0.7$.

critical value, and so it is unlikely that nearly neutral disturbances will ever be observed in a laboratory experiment. The wave number of the most unstable disturbance lies typically between 1 and 2 when the critical Rayleigh number is exceeded by more than a few per cent. Because of convergence difficulties in the expansion, the behavior for Couette flow has not been investigated in detail. Greater success was achieved in the case of an inclined layer [3], and the reader is referred to that paper for a more detailed discussion and for comparison with experimental observations. For comparison of theory and experiment in the case of wavy Taylor vortices the reader is referred to Eagles [24].

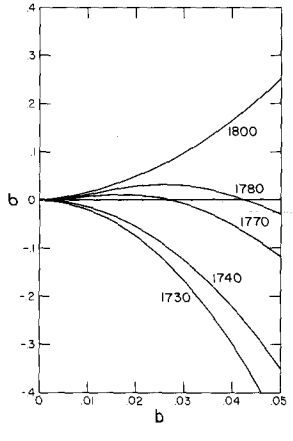

Figure 5
The dependence of the growth rate (σ) upon wavenumber (b) for various values of the Rayleigh number (wavy instability, $Re = 1000$).

The wavy instability of Taylor vortices is clearly related to the phenomenon of wavy convection rolls discussed here for Couette flow, even if the equations governing the two instabilities are different. From the point of view of verification of the neutral stability boundary, Taylor vortex flow is perhaps better suited. Although theory predicts that the minimum Taylor number (Ta) for secondary instability occurs as the circumferential wavenumber becomes zero ($Ta - Ta_c = 125$; see Eqn. (5.22) of [6]), the condition of circumferential periodicity places an additional constraint upon the possible wavenumbers and gives rise to the selection of an azimuthal wavenumber of at least unity at the onset of wavy vortices.

The behavior of the lower branch of the neutral curve for the wavy instability shown in Fig. 4 can be predicted by an expansion procedure valid for $(b\,Re) \ll 1$ and $(Ra-Ra_c)/Ra_c = \varepsilon^2 \ll 1$, both of which conditions are fulfilled in this region. As discussed in [3], the growth rate behaves in this limit as

$$\sigma = -b^2\{Re^2(A - \varepsilon^2 B) + \varepsilon^2 C\}. \tag{3.10}$$

The term involving A represents the damping of x-dependent disturbances for $Ra = Ra_c$, whereas the term involving C represents the damping of the wavy mode when $Re = 0$ and $\varepsilon^2 \ll 1$. The term involving B yields the wavy instability in such a way that, at $Re \gg 1$, the boundary is described approximately by the relation $\varepsilon_c^2 = (A/B)$. We emphasize that the wavy instability occurs for $(bRe) \ll 1$ so that a distinction can be made between this instability and lightly damped hydrodynamic disturbances which can exist for $b \to 0$ but with (bRe) fixed. For instance, Gallagher and Mercer [19] have shown that the decay rate of such disturbances has a local minimum (for a fixed value of b) somewhat below the bifurcation point which divides monotonically decaying disturbances from decaying oscillatory disturbances. However, the bifurcation point occurs as $b \to 0$ for $(bRe) \simeq 300$, which is far above the values used here to locate the neutral stability curve for the wavy instability.

As the reader will note in Fig. 4, the oscillatory neutral curve ends at a finite value of Re. Up to this value, the instability begins at a finite wavenumber (in the manner of Fig. 7(b) of [3]), where the decay rate (as a function of b) becomes zero. At the end of the curve in Fig. 4, σ_i for the most unstable disturbance vanishes, and the oscillatory instability merges with the wavy instability and another more stable nonoscillatory mode (in an analogous manner to the bifurcation which occurs in homogeneous Couette flow; see Fig. 1 of [19]).

The oscillatory instability is not related to any two-dimensional Tollmien–Schlichting type instability. Thus, the wavenumber b and a wave speed c based on the advective time-scale $(H/\Delta U_0^*)$ and obtained from

$$c = \sigma_i/(Re\,Pr\,b) \tag{3.11}$$

are plotted in Fig. 6. We note that both b and c decrease as Re increases, which is in contrast to the expected behavior of lightly damped solutions to the Orr–Sommerfeld

equation for Couette flow at large Re [20]. The matter of whether a hydrodynamic instability involving propagating waves can take place at higher values of Re is not addressed in this paper. We note that for $Re \gg Ra \gg 1$ and finite b, the momentum equations (3.6) become uncoupled from the energy equation (3.7), and the problem reduces to an investigation of the hydrodynamic stability of the nonplanar shear flow $\{z + U_1(y, z)\}$.

Finally, it should be mentioned that the neutral stability boundaries are sensitive to variations in Pr, as can be seen from the results for the inclined layer [3]. No secondary instabilities were observed in the high Pr experiments of Richter and Parsons [21], in which a Couette type apparatus was utilized (but with end walls, so that the laminar velocity profile was parabolic).

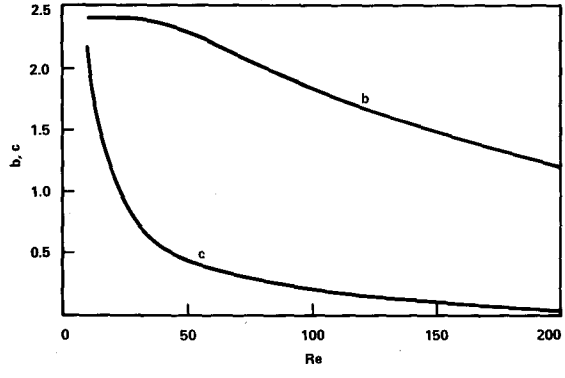

Figure 6
Wavenumber (b) and wavespeed (c) of the most unstable oscillatory disturbance as a function of the Reynolds number (Re) for $Pr = 0.7$.

4. The Disturbance Energy Balance

The disturbance energy equation has been investigated theoretically by Asai [22] and Lipps [18] for rolls and transverse waves in unstably stratified Couette flow, and LeMone [11] has discussed the energetics of atmospheric roll vortices on the basis of field data. Hence, we thought it worthwhile to present similar information for the secondary instability, at least for the wavy mode.

The equation for the mean kinetic energy of the disturbance is obtained by multiplying the linearized momentum equations (3.6) by the respective velocity components and then integrating over the entire layer. If we let $\langle \cdots \rangle$ denote an average obtained by such an integration, then the equation for the mean kinetic energy of the disturbance is

$$\frac{1}{Pr}\frac{d}{dt}\langle \tilde{u}^2 + \tilde{v}^2 + \tilde{w}^2 \rangle$$
$$= \left[Re \left\langle -\left(1 + \frac{d\bar{U}_1}{dz}\right)\tilde{u}\tilde{w} \right\rangle \right]_{\mathrm{I}} + \left[Ra\langle \theta \tilde{w} \rangle \right]_{\mathrm{II}}$$
$$\left[Re \left\langle -\left\{ \frac{\partial \tilde{U}_1}{\partial z}\tilde{u}\tilde{w} + \frac{\partial \tilde{U}_1}{\partial y}\tilde{u}\tilde{v} \right\} \right\rangle \right]_{\mathrm{III}}$$
$$+ \left[\frac{1}{Pr} \left\langle -\left\{ \frac{\partial V}{\partial y}\tilde{v}^2 + \frac{\partial V}{\partial z}\tilde{v}\tilde{w} \right.\right.\right.$$
$$\left.\left.\left. + \frac{\partial W}{\partial y}\tilde{w}\tilde{v} + \frac{\partial W}{\partial z}\tilde{w}^2 \right\} \right\rangle \right]_{\mathrm{IV}} - I_v, \tag{4.1}$$

where I_v is the dissipation integral. The various terms are normalized on the basis of I_v, so that I_v should be taken as unity in the following. The individual averages on the left-hand side have the following interpretations. The first average, $\langle \cdots \rangle_{\mathrm{I}}$, gives the transfer of energy into the disturbance from the mean shear flow, $z + \bar{U}_1(z)$, via a Reynolds stress. This would have been the only energy production term if we had done an analysis of the mean flow on the basis of the Orr–Sommerfeld equation. The second average represents the release of buoyant energy into kinetic energy and provides the coupling to the disturbance potential energy equation. The third average, $\langle \cdots \rangle_{\mathrm{III}}$, provides for energy transfer from the variable part of $U_1(y, z)$ via Reynolds stresses, whereas the fourth term allows for similar transfer from the velocity components $V(y, z)$ and $W(y, z)$ associated with the longitudinal rolls. In the limit of high Prandtl number, these latter terms become small, as does U_1.

The various averages in Eqn. (4.1) are given in Table 1. We list them in sequence as we come down along the upper branch of the neutral curve shown in Fig. 4 and then along the lower branch. All the terms are important initially but, as the minimum value of Re for instability is approached, terms I and II begin to predominate, with II being the main energy source (i.e., conversion of potential energy is relatively large). Once the minimum is reached, and we go along the lower branch, term I becomes increasingly large and becomes the dominant energy source as Re becomes large. This might suggest that a hydrodynamic instability associated with the distorted mean velocity profile, which has a point of inflection at $z = 0$, is the cause of the instability. However, it is clear that the numerical value of the mean vorticity is a minimum at $z = 0$ for values of Ra of interest, and so the flow is stable on an inviscid basis by the Fjørtoft-Høiland theorem [23, p. 105]. More fundamentally, we should remember that the wavy instability occurs first for values of $(bRe) \ll 1$, and, in this limit, Eqns. (3.6–3.8) are only weakly dependent upon U_1 and $\tilde{u}$. The strong dependence suggested by the results in Table 1 for the lower branch occurs because $\tilde{u}$ is driven somewhat passively by vorticity advection in the x-momentum equation, in much the same way that $U_1(y, z)$ is produced by the longitudinal rolls. It would therefore be misleading to use these results as a basis for a mechanistic explanation of the origin of the instability.

Table 1
Contributions to the mean disturbance kinetic energy equation for the neutrally stable, wavy mode (refer to Eqn. (4.1) for identification of the terms)

Re	*Ra*	I	II	III	IV
200	9500	0.225	0.295	−0.644	1.124
100	4500	0.275	0.508	0.186	0.031
50	2500	0.294	0.665	0.372	−0.332
40	2000	0.345	0.644	0.0945	−0.083
40	1880	0.395	0.599	0.0029	0.0031
50	1800	0.544	0.453	0.0017	0.0013
75	1775	0.738	0.260	0.0016	0.0006
100	1770	0.835	0.163	0.0016	0.0003
300	1765	0.977	0.021	0.0017	0.00005
1000	1765	0.996	0.0019	0.0020	0.00001
2000	1765	0.997	0.0005	0.0028	0.00001

$Re = (\Delta U_0^* H)/\nu$, $Ra = (g\alpha\Delta T_0^* H^3)/\nu\kappa$
where ν = kinematic viscosity,
κ = thermal diffusivity,
α = coefficient of thermal expansion.

Similar calculations have been made for the oscillatory instability. At the end of the stability curve ($Re \approx 200$; cf. Fig. (4)), terms I, II, and III predominate, with each being roughly equal.

Acknowledgement

This research was supported by the U.S. Army Research Office and by the National Science Foundation (Atmospheric Sciences Div.). A portion of the computing funds was provided by the Campus Computing Network at UCLA.

References

[1] R. E. Kelly, *The Onset and Development of Rayleigh-Bénard Convection in Shear Flows*, Proc. Int. Conf. on Physical Chemistry and Hydrodynamics (to be published by Hemisphere Publications Corp.).
[2] D. Avsec, *Sur les formes ondulées des tourbillons en bandes longitudinales*, Compt. Rend. Acad. Sci. *204*, 167–169 (1937).
[3] R. M. Clever and F. H. Busse, *Instabilities of Longitudinal Convection Rolls in an Inclined Layer*, J. Fluid Mech. *81*, 107–127 (1977).
[4] J. E. Hart, *Transition to a Wavy Vortex Regime in Convective Flow between Inclined Plates*, J. Fluid Mech. *48*, 265–271 (1971).
[5] D. Coles, *Transition in Circular Couette Flow*, J. Fluid Mech. *21*, 385–425 (1965).
[6] A. Davey, R. C. DiPrima, and J. T. Stuart, *On the Instability of Taylor Vortices*, J. Fluid Mech. *31*, 17–52 (1968).
[7] R. G. Fleagle, *Bomex: An Appraisal of Results*, Science *176*, 1079–1090 (1972).
[8] J. P. Kuettner, *Cloud Bands in the Earth's Atmosphere*, Tellus *23*, 404–425 (1971).
[9] R. Krishnamurti, *On Cellular Cloud Patterns. Part 3: Applicability of the Mathematical and Laboratory Models*, J. Atm. Sci. *32*, 1373–1383 (1975).
[10] R. A. Brown, *Analytical Methods in Planetary Boundary-Layer Modelling*, Adam Hilger Ltd., London (1974), pp. 94–119.
[11] M. A. LeMone, *The Structure and Dynamics of Horizontal Roll Vortices in the Planetary Boundary Layer*, J. Atm. Sci. *30*, 1077–1091 (1973).

[12] J. S. MALKUS and H. RIEHL, *Cloud Structure and Distribution over the Tropical Pacific Ocean*, Univ. California Press, Berkeley and Los Angeles (1964).
[13] H. L. KUO, *Perturbations of Plane Couette Flow in Stratified Fluid and Origin of Cloud Streets*, Phys. Fluids *6*, 195–211 (1963).
[14] J. KUETTNER, *The Band Structure of the Atmosphere*, Tellus *11*, 267–294 (1959).
[15] R. MARKSON, *Atmospheric Electrical Detection of Organized Convection*, Science *188*, 1171–1177 (1975).
[16] J. W. DEARDORFF, *Gravitational Instability between Horizontal Plates with Shear*, Phys. Fluids *8*, 1027–1030 (1965).
[17] R. M. CLEVER and F. H. BUSSE, *Transition to Time-Dependent Convection*, J. Fluid Mech. *65*, 625–645 (1974).
[18] F. B. LIPPS, *Two-Dimensional Numerical Experiments in Thermal Convection with Vertical Shear*, J. Atm. Sci. *28*, 3–19 (1971).
[19] A. P. GALLAGHER and A. MCD. MERCER, *On the Behavior of Small Disturbances in Plane Couette Flow*, J. Fluid Mech. *13*, 91–100 (1962).
[20] A. DAVEY, *On the Stability of Plane Couette Flow to Infinitesimal Disturbances*, J. Fluid Mech. *57*, 369–380 (1973).
[21] F. M. RICHTER and B. PARSONS, *On the Interaction of Two Scales of Convection in the Mantle*, J. Geophys. Res. *80*, 2529–2541 (1975).
[22] T. ASAI, *Three-Dimensional Features of Thermal Convection in a Plane Couette Flow*, J. Meteor. Soc. Japan *48*, 18–29 (1970).
[23] R. BETCHOV and W. O. CRIMINALE, Jr., *Stability of Parallel Flows*, Academic Press, New York (1967).
[24] P. M. EAGLES, *On the Torque of Wavy Vortices*, J. Fluid Mech. *62*, 1–9 (1974).

Summary

An investigation has been made of the instabilities of longitudinal convection rolls in a Couette flow which is heated from below. The instabilities occur either as stationary waves or as waves which propagate along the convection rolls. Neutral stability curves are presented as a function of Rayleigh and Reynolds numbers for a Prandtl number of 0.7. The disturbance energy budget is given for selected values of the Rayleigh and Reynolds numbers.

Zusammenfassung

Die Instabilitäten von longitudinalen Konvektionsrollen in einer ebenen Couette-Strömung, die von unten erhitzt wird, sind untersucht worden. Die Instabilitäten nehmen entweder die Form von stehenden Wellen an oder von Wellen, die sich entlang der Konvektionsrollen fortpflanzen. Die Kurven für marginale Stabilität sind als Funktion der Rayleigh- und Reynoldszahl dargestellt worden im Fall der Prandtlzahl 0.7. Das Energiebudget der Störungen wird für ausgewählte Werte der Rayleigh- und Reynoldszahl angegeben.

(Received: April 25, 1977)